Theory of time-resolved Raman scattering and fluorescence emission from semiconductor quantum dots

Julia Kabuss,[1,*] Stefan Werner,[2] Axel Hoffmann,[2] Peter Hildebrandt,[3] Andreas Knorr,[1] and Marten Richter[1]

[1]*Institut für Theoretische Physik, Nichtlineare Optik und Quantenelektronik, Technische Universität Berlin,
Hardenbergstraße 36, EW 7-1, D-10623 Berlin, Germany*

[2]*Institut für Festkörperphysik, Technische Universität Berlin, Hardenbergstraße 36, EW 5-1, D-10623 Berlin, Germany*

[3]*Max-Volmer-Laboratorium für Biophysikalische Chemie, Institut für Chemie, PC14, Technische Universität Berlin, Berlin, Germany*

We present a microscopic description of time-resolved Raman scattering and fluorescence emission of a coupled phonon-quantum dot system. Using density matrix formalism and higher-order Born approximation, the optical emission and scattering spectra of an InGaAs/GaAs-quantum dot are calculated for stationary and pulsed optical excitation. By means of their characteristic decay times, contributions such as Rayleigh, Raman, and fluorescence can be distinguished.

PACS number(s): 78.67.Hc, 78.47.jd, 78.30.−j

I. INTRODUCTION

Optical scattering experiments such as Raman and Rayleigh scattering on lower dimensional semiconductor nanostructures [quantum dots (QDs), quantum wells, nanotubes, etc.] result in a variety of different emission peaks and spectral features.[1–4] Besides direct elastic (Rayleigh) and inelastic scattering (Raman), electronic transitions between the different QD levels (fluorescence)[5,6] are induced. These different contributions to the emission can be discriminated by their characteristic spectral positions, when detuning the laser frequency.[7] The frequency ω_{k_s} of the scattered light either coincides with the excitation frequency (Rayleigh) or is shifted by a constant value (Raman), whereas the spectral positions of the fluorescence lines depend on the gap energy of the electronic system. Since these scattering contributions originate from different physical processes, described by different elements of the density matrix with its individual temporal dynamics and decay, they can also be distinguished by their specific temporal dynamics. The temporal dependence of various separate optical processes of QDs was examined experimentally as well as theoretically.[7–11] A common approach to describe the stationary fluorescence or Raman emission is via second-order perturbation theory.[12,13] The Raman cross section for stationary optical excitation is then given by the Kramers-Heisenberg expression.[14,15] Another approach, also leading to the stationary and dynamic Raman and fluorescence emission spectrum employs a density matrix formalism in Liouville space using third-order response functions.[7,16]

In this paper, we present a consistent approach, using a quantized description of the emission and scattering spectra, which does not only provide the frequency, but also the time-resolved Rayleigh, Raman, and fluorescence contributions of a semiconductor QD. In the stationary limit, the present approach gives an expression analogous to the Kramers-Heisenberg formula,[17] but it allows a consistent implementation of additional ultrafast and nonlinear interaction processes.

For the description of the quantum emission, we choose a perturbative approach to the density matrix, which allows the simultaneous description of time and frequency resolved Raman and fluorescence. The interaction of electrons with phonons and photons is incorporated microscopically. On the basis of the Heisenberg equation of motion, we derive a closed set of equations, using a correlation expansion technique.[18,19] This set is solved numerically and provides the emission and scattering spectra. The dynamics of the various optical processes are compared with the temporal behavior of material quantities and experimental parameters such as the excitation pulse. Our approach can easily be generalized to more complex systems including more states and interaction channels. To our knowledge, a correlation expansion approach, in order to describe time-resolved Raman and fluorescence emission of a semiconductor QD on a self-consistent footing has not yet been developed.

Starting with the Hamilton operator of the system in Sec. II, which describes the interaction of the QD with a phonon bath, the classical external and the quantized optical light field, an expression for the time-dependent emission spectrum is then defined in Sec. III. In Sec. IV, we derive the relevant equations of motion and discuss the physical meaning of expectation values representing measurable quantities. The results are finally analyzed in Sec. V.

II. HAMILTON OPERATOR

The Hamilton operator of the total system is given by $H = H_0 + H_{e-l} + H_{el-pt} + H_{el-pn}$. Here, H_0 represents the free energy of the photons, phonons (here approximated using the LO-bulk mode only) and the quasi-free-electronic motion. The other Hamiltonians describe the interaction of the quantum confined electrons with phonons H_{el-pn}, with the exciting laser field H_{e-l} and the photon field H_{el-pt} in rotating-wave approximation (RWA).[12] The applied Hamiltonians read,[20]

$$H_0 = \sum_\lambda \epsilon_\lambda a_\lambda^\dagger a_\lambda + \sum_\mathbf{k} \epsilon_k c_\mathbf{k}^\dagger c_\mathbf{k} + \sum_\mathbf{q} \epsilon_q b_\mathbf{q}^\dagger b_\mathbf{q}, \tag{1}$$

$$H_{el-pt} = \sum_\mathbf{k} \{ D_{cv}^\mathbf{k} a_c^\dagger a_v c_\mathbf{k} + D_{cv}^{\mathbf{k}*} a_v^\dagger a_c c_\mathbf{k}^\dagger \}, \tag{2}$$
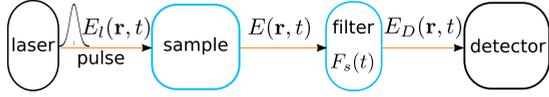
FIG. 1. (Color online) Measurement setup.

$$H_{\text{el-pn}} = \sum_{\mathbf{q}} \{g^{\mathbf{q}} a_c^\dagger a_c b_{\mathbf{q}} + g^{\mathbf{q}*} a_c^\dagger a_c b_{\mathbf{q}}^\dagger\}, \tag{3}$$

$$H_{e-1} = \mathbf{d}_{vc} \cdot \mathbf{E}(t) a_v^\dagger a_c + \mathbf{d}_{cv} \cdot \mathbf{E}(t) a_c^\dagger a_v. \tag{4}$$

The fermionic $a^{(\dagger)}$ and bosonic operators $b^{(\dagger)}$ and $c^{(\dagger)}$ are the creation and annihilation operators of the electrons, phonons, and photons. The free energies of the associated quantum states are $\epsilon_i = \hbar\omega_i$ are and q and k are the wave numbers of the phonon and photon system, respectively. For excitation near resonance and to illustrate our approach, we assume a small QD, which can be treated as a two-level system.[21] Here, v and c denote the electronic valence- and conduction-band states of the QD. The optical excitation of the QD is represented by the semiclassical electron field Hamiltonian H_{e-1}. The classical radiation field $\mathbf{E}(t)$ is described within the slowly varying amplitude-approximation, since the duration of the excitation pulses is long compared to the optical period. The microscopic dipole matrixelement for transitions between the lowest confined valence and conduction-band state is denoted as $\mathbf{d}_{cv}$. Since spontaneous emission is a quantum effect, the interaction of the emitted light with the electronic system is mediated by the quantized Hamiltonian $H_{\text{el-pt}}$,[20] including all photon modes with coupling matrix elements $D_{cv}^{\mathbf{k}}$. The description of the electron-phonon interaction is restricted to the interaction with the LO-phonon mode. Our method can in a straightforward way be extended to the interaction with other phonon modes. The electron-phonon interaction is described by $H_{\text{el-ph}}$ with the Fröhlich-coupling[19,22] matrix elements $g_{ii}^{\mathbf{q}}$. The initial conditions of the system were taken into account by introducing shifted operators $\tilde{b}_{\mathbf{q}} = b_{\mathbf{q}} + \alpha_{\mathbf{q}}$, where α is a complex number. This operator-transformation shifts the electronic energies $\tilde{\epsilon}_i = \epsilon_i - 2\sum_{\mathbf{q}} \frac{|g_{ii}^{\mathbf{q}} g_{jj}^{\mathbf{q}*}|}{\hbar\omega_{\mathbf{q}}}$ and relative coupling elements $g^{\mathbf{q}} = g_{cc}^{\mathbf{q}} - g_{vv}^{\mathbf{q}}$ and thus eliminates the coupling to the initial electronic equilibrium state to account for Born approximation.

III. OBSERVABLES

For a stationary external radiation field, the steady state emission of a specific mode $\mathbf{k}_s$ is given by[23]

$$S(\omega_{k_s}) = \partial_t n_{\mathbf{k}_s}, \tag{5}$$

where $n_{\mathbf{k}_s} = \langle c_{\mathbf{k}_s}^\dagger c_{\mathbf{k}_s} \rangle$ is the average photon number in the mode $\mathbf{k}_s$. However, for a time-dependent envelope of the electromagnetic field, e.g., a laser pulse, which is short or comparable to the time-resolution Δt of the detector, this expression cannot be used to calculate the spectrum. Instead, a time-resolved spectrum can be defined considering the specific experimental setup including a temporal gate,[24] cf. Fig. 1. The system is excited by a laser pulse and emits light $\mathbf{E}(\mathbf{r}, t)$, which here is described quantum optically. The field

$\mathbf{E}_D$, which hits the photodetector first gets spectrally filtered around a selected frequency ω_{k_s} with the band width $\Delta\omega$. The bandwidth product of the used filter then determines the simultaneous temporal resolution $\Delta\omega\Delta t$ of the measurement setup.

For an ideal filter such as the *spectral slit function*,[24] used for our calculations, the amplitude transmission function $F_{\omega_{k_s}}^{(0)}(t)$ and the spectral transmission function $\hat{F}(\omega_{k_s})$ are connected via Fourier transformation. Regarding only one polarization direction, without loss of generality in the far field, the filtered electromagnetic field is given by a convolution with the filtering function $F_s(t) = F_{\omega_{\mathbf{k}_s}}^{(0)} e^{i\omega_{k_s}t}$,

$$E_D(\mathbf{r},t) = \int_{-\infty}^{\infty} F_{\omega_{k_s}}(t - t') E(\mathbf{r},t') dt'. \tag{6}$$

We assume that the signal outside the sample is only detected around a small solid angle from the detector, so that here $\mathbf{k} \approx (0, k\mathbf{e}_z)$. The time and frequency-resolved spectrum $S(\mathbf{r}, \omega_{k_s}, t) = \langle E_D^{(-)}(\mathbf{r}, t) E_D^{(+)}(\mathbf{r}, t) \rangle$ is now given by the intensity at the detector at position $\mathbf{r}$.[25,26] Inserting Eq. (6) into the expression for the intensity gives

$$S(\mathbf{r}, \omega_{k_s}, t) = \int_{-\infty}^{\infty} dt_1 \int_{-\infty}^{\infty} dt_2 F_{\omega_{k_s}}^{(0)*}(t - t_1) F_{\omega_{k_s}}^{(0)}(t - t_2)$$
$$\times \langle E^{(-)}(\mathbf{r}, t_1) E^{(+)}(\mathbf{r}, t_2) \rangle$$
$$\times e^{-i\omega_{k_s}t_1} e^{i\omega_{k_s}t_2}. \tag{7}$$

To simplify Eq. (7), we follow here the approach of M. Kira *et al.*[25] Using, that the electric field is propagating freely between sample and detector in direction $\mathbf{r} = z\mathbf{e}_z$ i.e., $E^\pm(\mathbf{r}, t) = E^\pm(z - ct)$ and substituting integration variables according to $z_1 - ct = z - ct_1$ and $z_2 - ct = z - ct_2$ and assuming a Gaussian *amplitude transmission function* $F_{\omega_{k_s}}(\tau) = \exp(-(\frac{\tau}{\sqrt{2}\Delta t})^2)$ leads to

$$S(z\mathbf{e}_z, \omega_{k_s}, t) = \int_{-\infty}^{\infty} dz_1 \int_{-\infty}^{\infty} dz_2 e^{i\omega_{k_s}(z_1 - z)/c} e^{-i\omega_{k_s}(z_2 - z)/c}$$
$$\times \langle E^{(-)}(z_1 - ct) E^{(+)}(z_2 - ct) \rangle$$
$$\times e^{-[(z_2 - z)/\sqrt{2}\Delta t]^2} e^{-[(z_1 - z)/\sqrt{2}\Delta t]^2}. \tag{8}$$

Inserting the mode expansion $E^\pm(z - ct) = \sum_{\mathbf{k}} \sqrt{(\hbar\omega_k/2\epsilon_0 V)} e^{\pm i\mathbf{k}\cdot\mathbf{z}} c_{\mathbf{k}}^{(\dagger)}(t)$ for the electromagnetic field, the integrals can be solved and Eq. (7) reads

$$S(z\mathbf{e}_z, \omega_{k_s}, t) = \sum_{\mathbf{k}_1, \mathbf{k}_2} \hbar \frac{\sqrt{\omega_{k_1}\omega_{k_2}}}{2\epsilon_0 c^2 V} \langle c_{\mathbf{k}_1}^\dagger c_{\mathbf{k}_2} \rangle e^{-i(k_1 - k_2)z}$$
$$\times e^{-\{[(k_1 - k_s)c\Delta t]/\sqrt{2}\}^2} e^{-\{[(k_2 - k_s)c\Delta t]/\sqrt{2}\}^2}, \tag{9}$$

with $\omega_{k_i} = ck_i$. Here, the dynamic variables that need to be calculated in the following are the photon-coherences $\langle c_{\mathbf{k}_1}^\dagger c_{\mathbf{k}_2} \rangle$. In the stationary limit, the spectrum can be simplified to the form of Eq. (5). For very long optical pulses, the time-resolution of the setup can be chosen very large ($\Delta t \to \infty$). Since for a stationary light field $\langle E^{(-)}(\mathbf{r}, t' + \tau) E^{(+)}(\mathbf{r}, t') \rangle$ does not depend on t', Eq. (7) yields

$S(\omega_{k_s}, t) = \frac{\hbar \omega_{k_s}}{2\epsilon_0 c^2} n_{\mathbf{k}_s}$, with $S(\omega_{k_s}, t) \propto t$,[27] which was shown in Ref. 25. This formula is valid only for stationary pulses. In the quasistationary limit, e.g., the pulse width is larger than the resolution of the detector, the emission dynamics can be expected to be slow compared to the detector and Eq. (5) can be used to calculate the spectrum via the steady-state photon flux.[28]

IV. EQUATIONS OF MOTION

The emission spectrum will be calculated for pulsed excitation, so that the external laser field reads

$$\mathbf{E}_l(\mathbf{r}, t) = \mathbf{E}_l(t) e^{i\mathbf{k}_l \cdot \mathbf{r} - i\omega_l t} + \mathbf{E}_l^*(t) e^{-i\mathbf{k}_l \cdot \mathbf{r} + i\omega_l t}, \quad (10)$$

with a temporal envelope $\mathbf{E}_l(t)$. Using Heisenberg equations of motion $\partial_t \langle O \rangle = \frac{i}{\hbar}[H, O]$, a factorization of expectation values [see Eq. (18)] with a higher-order Born-approximation and bath assumption for the phonon field results in a closed set of coupled differential equations. In the following, this approach will be outlined and some of the relevant equations will be discussed.

In order to calculate the time-resolved emission spectrum with the help of Eq. (9), the dynamics of the photon coherences $\langle c_{\mathbf{k}_1}^\dagger c_{\mathbf{k}_2} \rangle$ must be known,

$$\partial_t \langle c_{\mathbf{k}_1}^\dagger c_{\mathbf{k}_2} \rangle = i(\omega_{k_1} - \omega_{k_2}) \langle c_{\mathbf{k}_1}^\dagger c_{\mathbf{k}_2} \rangle + \frac{i}{\hbar} D_{cv}^{\mathbf{k}_1} \langle a_c^\dagger a_v c_{\mathbf{k}_2} \rangle$$

$$- \frac{i}{\hbar} D_{cv}^{\mathbf{k}_2 *} \langle a_v^\dagger a_c c_{\mathbf{k}_1}^\dagger \rangle. \quad (11)$$

The photon coherences are driven by photon-assisted polarizations $\langle a_i^\dagger a_j c_{\mathbf{k}_n}^{(\dagger)} \rangle$, which themselves couple to higher order many-particle correlations. The equation of motion for the first source term in Eq. (11) is given by

$$\partial_t \langle a_c^\dagger a_v c_{\mathbf{k}} \rangle = -i(\omega_k - \omega_{cv} - i\gamma) \langle a_c^\dagger a_v c_{\mathbf{k}} \rangle - \frac{i}{\hbar} D_{cv}^{\mathbf{k}*} f_c$$

$$+ \frac{i}{\hbar} \sum_{\mathbf{q}} \{ g_{vc}^{\mathbf{q}} \langle a_c^\dagger a_v b_{\mathbf{q}} c_{\mathbf{k}} \rangle + g_{vc}^{\mathbf{q}*} \langle a_c^\dagger a_v b_{\mathbf{q}}^\dagger c_{\mathbf{k}} \rangle \}$$

$$+ \frac{i}{\hbar} \mu_{vc}^+ [\langle a_v^\dagger a_v c_{\mathbf{k}} \rangle_{1+} - \langle a_c^\dagger a_c c_{\mathbf{k}} \rangle_{1+}], \quad (12)$$

with $\langle a_i^\dagger a_i c_{\mathbf{k}} \rangle_{n\pm} = \langle a_i^\dagger a_i c_{\mathbf{k}} \rangle e^{\pm ni\omega_l t}$ and $(n \in \mathbb{N})$, introducing the abbreviation $f_c = \langle a_c^\dagger a_c \rangle$ for the conduction band density. To account for other many-particle interactions, a pure dephasing constant γ is added phenomenologically in the equations for the polarizations.[19,29] For Eq. (12) the following notation was used,

$$\hbar \Omega_{ij} = \mathbf{E}(t) \cdot \mathbf{d}_{ij}$$

$$= d_{ij}^+ E(t) e^{i\mathbf{k}\cdot\mathbf{r} + i\omega_l t} + d_{ij}^- E(t) e^{i\mathbf{k}\cdot\mathbf{r} - i\omega_l t}$$

$$\equiv \mu_{ij}^+(t) e^{i\omega_l t} + \mu_{ij}^-(t) e^{-i\omega_l t}. \quad (13)$$

$\mu_{ij}^\pm$ contains the phase $e^{\mp i\mathbf{k}\cdot\mathbf{r}}$, the temporal envelope of the electromagnetic field, and the microscopic dipole matrix element between the QD levels i and j. In the following, the

rapid oscillation contributions are split off and transferred to the expectation values,

$$\hbar \Omega_{ni} \langle a_m^\dagger a_j A \rangle = \mu_{ni}^+ e^{i\omega_l t} \langle a_m^\dagger a_j A \rangle + \mu_{ni}^- e^{-i\omega_l t} \langle a_m^\dagger a_j A \rangle$$

$$\equiv \mu_{ni}^+ \langle a_m^\dagger a_j A \rangle_{1+} + \mu_{ni}^- \langle a_m^\dagger a_j A \rangle_{1-}, \quad (14)$$

where A is an arbitrary bosonic ladder operator. Furthermore, the system was assumed to be excited near resonance, so that a RWA could be applied to Eq. (14); if $\langle O \rangle$ is a slowly rotating quantity,

$$\hbar \Omega_{ij} \langle O \rangle_{1+} \approx \mu_{ij}^- \langle O \rangle_{0+} + \mu_{ij}^+ \langle O \rangle_{2+}, \quad (15)$$

$$\hbar \Omega_{ij} \langle O \rangle_{1-} \approx \mu_{ij}^+ \langle O \rangle_{0-} + \mu_{ij}^- \langle O \rangle_{2-}. \quad (16)$$

If $\langle O \rangle$ is a polarizationlike quantity, the last term of either Eq. (15) or Eq. (16) has to be considered. Quantum corrections (double photon-assisted correlations) to the induced emission have been disregarded in Eq. (12), because of negligible photon numbers in the quantum optical modes.

Deriving the required equations of motion [Eqs. (11) and (A12)] will result in different source terms to the emission. There are several contributions to the spectrum, which originate from two physically different mechanisms. On the one hand, there are direct coherent scattering processes, where the incoming photon is scattered either elastically (Rayleigh) or under emission/absorption of a phonon (Raman-Stokes/anti-Stokes). The latter process leads to a red ($\omega_{k_s} = \omega_l - \omega_{LO}$) or blue shift ($\omega_{k_s} = \omega_l + \omega_{LO}$) of the scattered photon to the Rayleigh line ($\omega_{k_s} = \omega_l$). On the other hand, there are sequential fluorescence processes, where the coherence is destroyed and a real population of an excited QD state, followed by emission of a photon at the band-gap energy $\omega_{k_s} = \omega_{cv}$. Through the coupling to the phonons, this fluorescence process can also occur under emission or absorption of a phonon. Therefore, also the fluorescence line will have satellite peaks in the lower and higher frequency range ($\omega_{k_s} = \omega_{cv} \mp \omega_{LO}$).

Starting with the source terms in Eq. (11), i.e., $\langle a_c^\dagger a_v c_{\mathbf{k}} \rangle = \langle a_v^\dagger a_c c_{\mathbf{k}}^\dagger \rangle^*$, we can refer to these expectation values as fluorescence terms. They are illustrated in Fig. 2, where resonances at the band-gap energy ($\omega_{k_s} = \omega_{cv}$) can be seen from
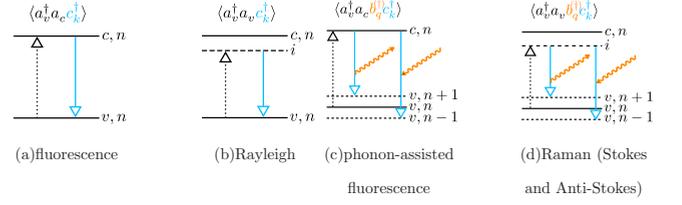
FIG. 2. (Color online) Operator scheme: straight arrows correspond to photon operators ($c_{\mathbf{k}}^\dagger$: emission of a photon), where the length of the straight arrows stands for the energy of the emitted photon. The expectation values correspond to the probability of the processes, depicted by the straight arrows on the right in each subfigure. Curved arrows stand for phonons $b_{\mathbf{q}}/b_{\mathbf{q}}^\dagger$. Within a phonon-assisted process, the energy of the emitted photon can be redshifted ($b^\dagger$: phonon-emission) or blueshifted (b: phonon absorption) with respect to the unperturbed process.

the free-energy rotation term, Eq. (12). Next to the driving external laser field coupled quantities and phonon-assisted quantities, Eq. (12) is driven by the c-band density f_c, which enters the equation via the el-pt coupling $D_{cv}^{\mathbf{k}*}$. This is due to the fact, that within a fluorescence process, a population in the upper QD level is built up. This excited QD state then decays, while the system emits a photon at the band-gap energy. Additionally, the many-particle operator combinations can be used to tell, if an operator quantity can be referred to as a (phonon-assisted) scattering or a fluorescence process, see Fig. 2. For example, Fig. 2(a) shows the fluorescence emission, related to the f_c contribution in Eq. (12). An electron in the c-band state is annihilated (a_c), while an electron in the v-band state is created ($a_v^\dagger$), describing a transition of the electron from the conduction band state to the valence band state. In this process, a photon in the mode $\mathbf{k}$ is emitted, which is described by the operator ($c_{\mathbf{k}}^\dagger$). This corresponds to an emission process, where the electron relaxes into the ground state, emitting a photon with a frequency, depending on the free-energy rotation terms. Equation (12) contains the sources of different emission mechanisms, including Rayleigh scattering $\langle a_v^\dagger a_v c_{\mathbf{k}}\rangle_{1+}$, or phonon-assisted fluorescence emission $\langle a_c^\dagger a_v b_{\mathbf{q}}^\dagger c_{\mathbf{k}}\rangle$. This can be seen, if we analyze the dynamics of the different source terms.

(i) The dynamics of the resonance fluorescence emission is determined by f_c [Eq. (12)], which gives the probability for the occupation of the upper QD level. It is incorporated into the equation via the interaction ($D_{cv}^{\mathbf{k}}$) with the quantum optical field modes,

$$\partial_t f_c = \frac{i}{\hbar}\sum_{\mathbf{k}}\{D_{cv}^{\mathbf{k}}\langle a_v^\dagger a_c c_{\mathbf{k}}^\dagger\rangle + D_{cv}^{\mathbf{k}}\langle a_c^\dagger a_v c_{\mathbf{k}}\rangle\}$$
$$+ \frac{i}{\hbar}[\mu_{vc}^+\rho_{vc}^+ - \mu_{cv}^-\rho_{vc}^{+*}], \qquad (17)$$

with the microscopic polarization $\rho_{vc}^+ = \langle a_v^\dagger a_c\rangle e^{i\omega_l t}$. Due to the coupling to the quantum optical field modes, a radiative dephasing is consistently provided by our approach. Since the conduction-band density f_c is directly connected to the fluorescence emission [see Eq. (12) and Fig. 2(a)], the dynamics of the fluorescence peak is determined by the radiative life time.

(ii) The equations of motion for the photon and phonon-assisted polarizations $\langle a_i^\dagger a_j b_{\mathbf{q}}^{(\dagger)} c_{\mathbf{k}}\rangle$ are similar to Eq. (12), describing phonon-assisted fluorescence processes. Again, the spectral positions of the resonances are to be read off the free-energy rotation in Eqs. (A1) and (18), giving the satellite peaks in the spectral distance of a LO-phonon energy ($\omega_k = \omega_{cv} \mp \omega_{\mathbf{q}}$). Figure 2(c) schematically shows the associated process, using the ladder-operators for interpretation,

$$\partial_t\langle a_c^\dagger a_v b_{\mathbf{q}}^\dagger c_{\mathbf{k}}\rangle = -i(\omega_k - \omega_{cv} - \omega_{\mathbf{q}} - i\gamma)\langle a_c^\dagger a_v b_{\mathbf{q}}^\dagger c_{\mathbf{k}}\rangle$$
$$+ \frac{i}{\hbar}g_{vc}^{\mathbf{q}}[n_{\mathbf{q}} + 1]\langle a_c^\dagger a_v c_{\mathbf{k}}\rangle + \frac{i}{\hbar}\mu_{vc}^+[\langle a_v^\dagger a_v b_{\mathbf{q}}^\dagger c_{\mathbf{k}}\rangle_{1+}$$
$$- \langle a_c^\dagger a_c b_{\mathbf{q}}^\dagger c_{\mathbf{k}}\rangle_{1+}] - \frac{i}{\hbar}D_{cv}^{\mathbf{k}*}\langle a_c^\dagger a_c b_{\mathbf{q}}^\dagger\rangle. \qquad (18)$$

Just like $\langle a_c^\dagger a_v c_{\mathbf{k}}\rangle$, these expectation values are driven by

densites $\langle a_c^\dagger a_c b_{\mathbf{q}}^\dagger\rangle$, so that the temporal behavior of the corresponding emission processes is determined by a radiative damping. Due to the many-particle character of the Hamiltonian, the set of equations cannot be closed, as each expectation value couples to expectation values of higher-order (creation and annihilation) operator correlations. Therefore, the resulting hierarchy problem[18,19,30] is closed via a factorization of the electron, photon and phonon operators according to

$$\langle a^\dagger a b^\dagger b(c^{(\dagger)})\rangle = \langle b^\dagger b\rangle\langle a^\dagger a(c^{(\dagger)})\rangle \approx n_{\mathbf{q}}\langle a^\dagger a(c^{(\dagger)})\rangle. \qquad (19)$$

using a second order Born approximation with respect to phonon operators.[18,31] Further on, the phonons are treated as a bath, such that the phonon modes remain in thermal equilibrium, i.e., $n_{\mathbf{q}} = \langle b_{\mathbf{q}}^\dagger b_{\mathbf{q}}\rangle = 1/[\exp(\hbar\omega_l/k_B T) - 1]$.[29]

(iii) The equation for one of the photon-assisted densities $\langle a_v^\dagger a_v c_{\mathbf{k}}\rangle_{1+} = \langle a_v^\dagger a_v c_{\mathbf{k}}\rangle e^{i\omega_l t}$ in Eq. (12) reads

$$\partial_t\langle a_v^\dagger a_v c_{\mathbf{k}}\rangle_{1+} = -i(\omega_k - \omega_l)\langle a_v^\dagger a_v c_{\mathbf{k}}\rangle_{1+} - \frac{i}{\hbar}D_{cv}^{\mathbf{k}*}\rho_{vc}^+$$
$$+ \frac{i}{\hbar}[\mu_{cv}^-\langle a_c^\dagger a_v c_{\mathbf{k}}\rangle - \mu_{vc}^+\langle a_v^\dagger a_c c_{\mathbf{k}}\rangle_{2+}]. \qquad (20)$$

Due to the positive frequency component $e^{i\omega_l t}$ of the external laser field, which is included in the quantity $\langle a_v^\dagger a_v c_{\mathbf{k}}\rangle_{1+} = \langle a_v^\dagger a_v c_{\mathbf{k}}\rangle e^{i\omega_l t}$, the laser-frequency ω_l is contained in the free-energy rotation of Eq. (20). Unlike the quantities in Eqs. (12), (A1), and (18), $\langle a_v^\dagger a_v c_{\mathbf{k}}\rangle_{1+}$ couples directly to the quantum optical field modes via the microscopic polarization ρ_{vc}^+,

$$\partial_t\rho_{vc}^+ = -i(\omega_{cv} - \omega_l - i\gamma)\rho_{vc}^+ + \frac{i}{\hbar}\Bigg\{\sum_{\mathbf{k}}D_{cv}^{\mathbf{k}}\langle a_c^\dagger a_c c_{\mathbf{k}}\rangle_{1+}$$
$$- D_{cv}^{\mathbf{k}}\langle a_v^\dagger a_v c_{\mathbf{k}}\rangle_{1+}\Bigg\} - \frac{i}{\hbar}\sum_{\mathbf{q}}\{g_{vc}^{\mathbf{q}}\langle a_v^\dagger a_c b_{\mathbf{q}}\rangle_{1+}$$
$$+ g_{vc}^{\mathbf{q}*}\langle a_v^\dagger a_c b_{\mathbf{q}}^\dagger\rangle_{1+}\} + \frac{i}{\hbar}\mu_{cv}^-[2f_c - 1]. \qquad (21)$$

The temporal evolution of ρ_{vc}^+ is determined by the dynamics of the excitation pulse, which therefore defines the dynamics of the Rayleigh scattering line, Eq. (20).

(iv) Raman scattering can be related to a quantity such as the phonon and photon-assisted density $\langle a_v^\dagger a_v b_{\mathbf{q}} c_{\mathbf{k}}\rangle_{1+}$, which appears as a source term to the phonon-assisted polarization via the el-l- coupling in Eq. (22). Here we find a resonance line at a scattered frequency $\omega_k = \omega_l + \omega_{\mathbf{q}}$ [Eq. (22)] or $\omega_k = \omega_l - \omega_{\mathbf{q}}$ [Eq. (A4)] respectively. Like in the Rayleigh process, the electron is elevated into a virtual intermediate state i, which decays with the constitution of a population. Within this process, a photon of the laser energy plus/minus a phonon energy is emitted, see Fig. 2(d),

$$\partial_t\langle a_v^\dagger a_v b_{\mathbf{q}}^\dagger c_{\mathbf{k}}\rangle_{1+} = -i(\omega_k - \omega_l - \omega_{\mathbf{q}})\langle a_v^\dagger a_v b_{\mathbf{q}}^\dagger c_{\mathbf{k}}\rangle_{1+}$$
$$+ \frac{i}{\hbar}[\mu_{cv}^-\langle a_c^\dagger a_v b_{\mathbf{q}}^\dagger c_{\mathbf{k}}\rangle - \mu_{vc}^+\langle a_v^\dagger a_c b_{\mathbf{q}}^\dagger c_{\mathbf{k}}\rangle_{2+}]$$
$$- \frac{i}{\hbar}D_{cv}^{\mathbf{k}*}\langle a_v^\dagger a_c b_{\mathbf{q}}^\dagger\rangle_{1+}. \qquad (22)$$

TABLE I. Numerical parameters: e_0 denotes the elementary charge and m_0 denotes the electron mass.

Parameter	Symbol	Value
c-band effective mass	m_c	$0.043m_0$ [a]
v-band effective mass	m_v	$0.450m_0$ [a]
c-band oscillator energy	$\hbar\omega_c$	50 meV
v-band oscillator energy	$\hbar\omega_v$	25 meV
High-frequency dielectric constant	ε_∞	10.9[a]
Static dielectric constant	ε_s	12.53[a]
LO phonon energy	$\hbar\omega_{LO}$	36.4 meV[a]
Dipole moment	d_{vc}	$0.6e_0$ nm [b]
Pulse area	N	1

[a]Reference 32.
[b]Reference 9.

Like for the Rayleigh source terms in Eq. (12), the resonance terms for the Raman scattering, for example, $\langle a_v^\dagger a_v b_{\mathbf{q}} c_{\mathbf{k}} \rangle_{1+}$, enter the interaction chain via coupling to the external laser field. Thus, the Raman process is restricted to the duration of the square of the excitation pulse. Also, this quantity couples directly to a (phonon-assisted) polarization. The equation has different sources, but the quantity, relevant for the dynamics of the scattering enters via the el-pt coupling. The remaining equations of motion, necessary to calculate the equations for the photon coherences are discussed in the Appendix.

To summarize this section, we note that within the developed set of equations of motion, we are able to locate the sources to the emission: (i) resonance fluorescence, (ii) phonon-assisted fluorescence, (iii) Rayleigh scattering, and (iv) Raman scattering within a consistent description. Furthermore, the equations of motion a given in a scheme, compatible to ordinary cluster expansion and thus extendable to other semiconductor nanostructures.

V. DISCUSSION

The numerical results for the stationary and time-resolved emission spectrum, calculated on the basis of the equations of motion in Sec. IV and the Appendix, are shown and discussed in this section. For the calculations, the parameters for the el-pn, el-l, and el-pt coupling where taken according to Table I.

The fluorescence emission is associated with a real occupation of the conduction band state [Eq. (17)], which decays spontaneously. Thus, the fluorescence emission dynamics is determined by the lifetime of the upper level. Rayleigh and Raman scattering are expected to coincide with the dynamics and spectral properties of the exciting laser field, since their sources enter the interaction chain via coupling to the laser field [see Eqs. (12) and (18)].

In order to investigate the dynamics of the different contributions to the spectrum, excitation pulses (Gaussian), centered at 8 ps with a full width at half maximum (FWHM) of 2 ps and a spectral detuning of 20 meV from the band-gap energy, are taken for the calculations. Describing the temporal evolution of the different scattering emission parts, the
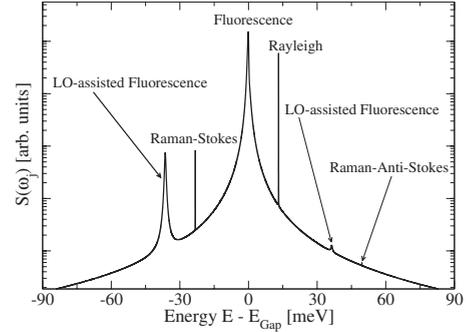

FIG. 3. Photon flux as calculated with Eq. (5) for excitation with a stationary laser pulse at $T=77$ K.

time resolution of the Gaussian filter function $F_s(t)$ is chosen to be fast ($\Delta t=400$ fs) in comparison to the dynamics of the excitation pulse, so that even the dynamics of the Rayleigh and Raman lines can be resolved.[25]

In Fig. 3 the spectrum is calculated via the photon flux [Eq. (5)] for the limit of a stationary light field. The spectrum is plotted versus the scattered minus the band-gap energy $\hbar(\omega_k - \omega_{cv})$, so that the main fluorescence peak appears at 0 eV. At ∓36.4 meV, there are LO-satellite peaks, which can be referred to as phonon-assisted fluorescence contributions [see Eqs. (18) and (A1)]. As stated in Sec. IV, the coherent Rayleigh-scattering line occurs at the laser frequency and is displaced by 20 meV with respect to the electronic transition energy ω_{cv}. The free-energy rotation of Eq. (20) determines the position of the according resonance, which appears at a scattered energy of $\hbar\omega_k = \hbar\omega_l$, i.e., the exciting laser energy. The Raman-Stokes and anti-Stokes scattering lines are separated from the laser energy by a LO-phonon energy ∓36.4 meV [see Eqs. (22) and (A4)]. The line shape of the incoherent fluorescence emission lines is determined by a pure dephasing.[19,29,33] The Rayleigh and Raman scattering lines are much sharper because of the large temporal width of the stationary excitation pulse.

Figure 4 shows the pulse-excited frequency resolved emission spectrum at different times after the excitation, as calculated with Eq. (7). The Rayleigh contribution performs
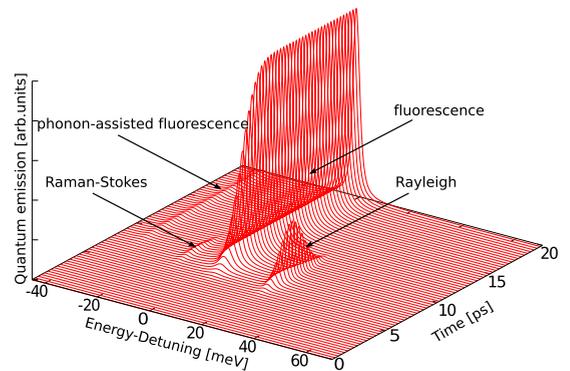

FIG. 4. (Color online) Time-resolved emission spectrum of an InGaAs/GaAs-QD after excitation with a coherent Gaussian pulse with 2 ps temporal width. The spectrum is plotted between 0 and 20 ps at a temperature of 77 K and time resolution of $\Delta t=400$ fs. The main fluorescence peak at the band gap energy is set to 0 meV.
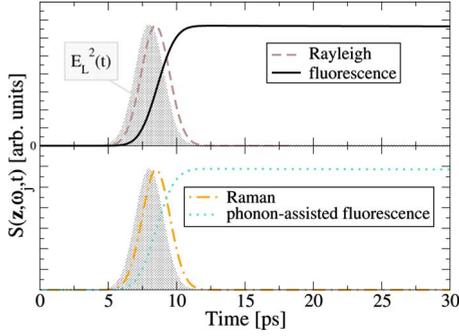
FIG. 5. (Color online) Time evolution of the fluorescence (solid line), Stokes-phonon replica (dotted line), Rayleigh (dashed line), and Raman (dotted-dashed line) scattering contributions under excitation with a laser pulse (FWHM of 2 ps). For comparison, Rayleigh and fluorescence as well as the phonon-assisted processes are normed to one height, respectively.

a Gaussian-shaped rise and decay in the spectral as well as in the temporal region. This is the result of the fast dynamics of the excitation pulse and the microscopic polarization ρ_{vc}^{+}. The Raman-Stokes and anti-Stokes scattering lines show the same temporal behavior as the Rayleigh line. Regarding the source terms of Eqs. (12), (18), and (A1) shows, that the Rayleigh and Raman resonance sources $\langle a_v^{\dagger} a_v (b_{\mathbf{q}}^{(\dagger)}) c_{\mathbf{k}} \rangle$ and $\langle a_c^{\dagger} a_c (b_{\mathbf{q}}^{(\dagger)}) c_{\mathbf{k}}^{\dagger} \rangle$ vanish together with the excitation pulse. Thus, the coherent Rayleigh and Raman scattering processes are only present, when the excitation pulse is nonzero. After the polarization has been destroyed and a population density has been built up, only the sequential fluorescence processes are left. The main resonance fluorescence line at the band-gap energy, which again was set to 0 meV and its satellites at ∓ 36.4 meV, rise until the polarization has decayed completely. Afterwards, they decrease due to the radiative damping of the conduction-band density. This is also illustrated in Figs. 5 and 6, depicting the temporal evolution of the different emission and scattering contributions and the behavior of the conduction-band density versus the polarization. Below 9 ps, the spectrum is dominated by the Raman and Rayleigh scattering lines. After several picoseconds, when the excitation pulse decays, the spectrum is dominated by the resonant fluorescence and the phonon-assisted fluorescence emission. Due to the finite resolution of the filter, the coherent scatter-
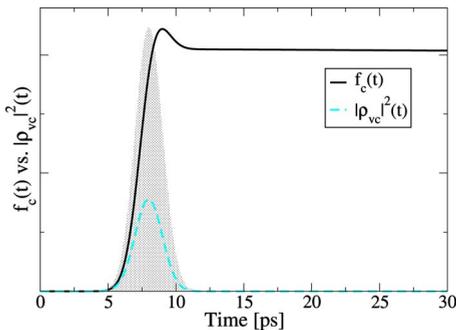
ing contributions are slightly retarded to the excitation pulse and the microscopic polarization ρ_{vc}.

Figures 3 and 4 show, that the anti-Stokes lines are weak compared to the Stokes emission and scattering lines. The blueshifted lines are dependent on the average phonon number $n_{\mathbf{q}}$, while redshifted lines come along with spontaneous phonon emission $n_{\mathbf{q}}+1$.

The quantities defining the emission and scattering dynamics enter the equations of motion via coupling to the quantum optical modes. Thus, the spectral and temporal emission behavior can be understood from the equations, which can be related to certain emission and scattering processes by interpreting the action of the ladder operator combinations. From Eq. (12), (A1), and (18) it can be seen that the terms, relevant for the resonance and phonon-assisted fluorescence emission, depend on the population of the conduction band level f_c and $\langle a_c^{\dagger} a_c b_{\mathbf{q}}^{(\dagger)} \rangle$. The conduction-band density decays radiatively, due to spontaneous emission, which determines the temporal behavior of the emission lines. The fluorescence emission parts in Fig. 5 show a decay behavior, which is comparable to the temporal evolution of the conduction band density, as plotted in Fig. 6. In contrast, the Raman and Rayleigh contributions from Eqs. (20), (22), and (A4) are not determined by the time evolution of densities, but by the temporal behavior of the classical excitation pulse and the microscopic polarizations, respectively. Their lineshapes, however, are connected to the decay of the conduction band density and the duration of FWHM of the pulse.

VI. CONCLUSION

In conclusion, a correlation expansion approach to the density matrix can be used to describe the temporal dynamics of light emission, including all relevant contributions, such as resonance and phonon-assisted fluorescence as well as Rayleigh and Raman scattering. The method is illustrated for a two-level semiconductor QD, coupled to LO-phonons. Since the description treats all contributions on an equal microscopic level, the evaluated emission dynamics can be used to discriminate the different scattering contributions in experiments. In prospective, our model can be generalized and adjusted to experiments that refer to more complex systems.[11] Typical examples will include the incorporation of relaxation or incoherent contributions to the time-resolved Raman linewidth.

ACKNOWLEDGMENTS

FIG. 6. (Color online) Time evolution of the conduction-band density (solid line) and the square of the microscopic polarization (dashed line).

APPENDIX: EQUATIONS OF MOTION

Many of the following equations resemble equations of Sec. III so that they are only briefly discussed. Equation (A1) describes a phonon-assisted fluorescence process [Fig. 2(c)],

$$\partial_t \langle a_c^\dagger a_v b_{\mathbf{q}} c_{\mathbf{k}} \rangle = -i(\omega_k - \omega_{cv} + \omega_{\mathbf{q}} - i\gamma)\langle a_c^\dagger a_v b_{\mathbf{q}} c_{\mathbf{k}} \rangle$$
$$+ \frac{i}{\hbar}\mu_{vc}^+[\langle a_v^\dagger a_v b_{\mathbf{q}} c_{\mathbf{k}} \rangle_{1+} - \langle a_c^\dagger a_c b_{\mathbf{q}} c_{\mathbf{k}} \rangle_{1+}]$$
$$- \frac{i}{\hbar}D_{cv}^{\mathbf{k}*}\langle a_c^\dagger a_c b_{\mathbf{q}} \rangle + \frac{i}{\hbar}g_{vc}^{\mathbf{q}*}n_{\mathbf{q}}\langle a_c^\dagger a_v c_{\mathbf{k}} \rangle. \quad (A1)$$

The remaining Rayleigh and Raman resonance terms are given by Eqs. (A2)–(A4), respectively. They are similar to Eqs. (20) and (22).

$$\partial_t \langle a_c^\dagger a_c c_{\mathbf{k}} \rangle_{1+} = -i(\omega_k - \omega_l)\langle a_c^\dagger a_c c_{\mathbf{k}} \rangle_{1+} + \frac{i}{\hbar}[\mu_{vc}^+\langle a_v^\dagger a_c c_{\mathbf{k}} \rangle_{2+}$$
$$- \mu_{cv}^-\langle a_c^\dagger a_v c_{\mathbf{k}} \rangle], \quad (A2)$$

$$\partial_t \langle a_c^\dagger a_c b_{\mathbf{q}} c_{\mathbf{k}} \rangle_{1+} = -i(\omega_k - \omega_l + \omega_{\mathbf{q}})\langle a_c^\dagger a_c b_{\mathbf{q}} c_{\mathbf{k}} \rangle_{1+}$$
$$+ \frac{i}{\hbar}[\mu_{vc}^+\langle a_v^\dagger a_c b_{\mathbf{q}} c_{\mathbf{k}} \rangle_{2+} - \mu_{cv}^-\langle a_c^\dagger a_v b_{\mathbf{q}} c_s \rangle]$$
$$- \frac{i}{\hbar}g_{vc}^{\mathbf{q}*}\langle a_c^\dagger a_c c_{\mathbf{k}} \rangle_{1+}, \quad (A3)$$

$$\partial_t \langle a_v^\dagger a_v b_{\mathbf{q}} c_{\mathbf{k}} \rangle_{1+} = -i(\omega_k - \omega_l + \omega_{\mathbf{q}})\langle a_v^\dagger a_v b_{\mathbf{q}} c_{\mathbf{k}} \rangle_{1+}$$
$$+ \frac{i}{\hbar}[\mu_{cv}^-\langle a_c^\dagger a_v b_{\mathbf{q}} c_s \rangle - \mu_{vc}^+\langle a_v^\dagger a_c b_{\mathbf{q}} c_{\mathbf{k}} \rangle_{2+}]$$
$$- \frac{i}{\hbar}D_{cv}^{\mathbf{k}*}\langle a_v^\dagger a_c b_{\mathbf{q}} \rangle_{1+}, \quad (A4)$$

$$\partial_t \langle a_c^\dagger a_c b_{\mathbf{q}}^\dagger c_{\mathbf{k}} \rangle_{1+} = -i(\omega_k - \omega_l - \omega_{\mathbf{q}})\langle a_c^\dagger a_c b_{\mathbf{q}}^\dagger c_{\mathbf{k}} \rangle_{1+}$$
$$+ \frac{i}{\hbar}[\mu_{vc}^+\langle a_v^\dagger a_c b_{\mathbf{q}}^\dagger c_{\mathbf{k}} \rangle_{2+} - \mu_{cv}^-\langle a_c^\dagger a_v b_{\mathbf{q}}^\dagger c_s \rangle]$$
$$+ \frac{i}{\hbar}g_{vc}^{\mathbf{q}}\langle a_c^\dagger a_c c_{\mathbf{k}} \rangle_{1+}. \quad (A5)$$

The action of the ladder operators of these quantities are depicted in Figs. 2(b) and 2(d). Equations (A5) and (A7) are comparable to the equation of the conduction-band density,

$$\partial_t \langle a_c^\dagger a_c b_{\mathbf{q}} \rangle = -i\omega_{\mathbf{q}}\langle a_c^\dagger a_c b_{\mathbf{q}} \rangle - \frac{i}{\hbar}g_{vc}^{\mathbf{q}*}f_c + \frac{i}{\hbar}\sum_{\mathbf{k}}\{D_{cv}^{\mathbf{k}*}\langle a_v^\dagger a_c b_{\mathbf{q}} c_{\mathbf{k}}^\dagger \rangle$$
$$- D_{cv}^{\mathbf{k}}\langle a_c^\dagger a_v b_{\mathbf{q}} c_{\mathbf{k}} \rangle\} + \frac{i}{\hbar}[\mu_{vc}^+\langle a_v^\dagger a_c b_{\mathbf{q}} \rangle_{1+}$$
$$- \mu_{cv}^-\langle a_c^\dagger a_v b_{\mathbf{q}} \rangle^-], \quad (A6)$$

$$\partial_t \langle a_v^\dagger a_v b_{\mathbf{q}} \rangle = -i\omega_{\mathbf{q}}\langle a_v^\dagger a_v b_{\mathbf{q}} \rangle + \frac{i}{\hbar}\sum_{\mathbf{k}}\{D_{cv}^{\mathbf{k}}\langle a_c^\dagger a_v b_{\mathbf{q}} c_{\mathbf{k}} \rangle$$
$$- D_{cv}^{\mathbf{k}*}\langle a_v^\dagger a_c b_{\mathbf{q}} c_{\mathbf{k}}^\dagger \rangle\} + \frac{i}{\hbar}[d_{cv}^-\langle a_c^\dagger a_v b_{\mathbf{q}} \rangle_-$$
$$- d_{vc}^+\langle a_v^\dagger a_c b_{\mathbf{q}} \rangle_{1+}]. \quad (A7)$$

These equations define the temporal evolution of the phonon-assisted fluorescence emission lines.

The strength of the signal, which depends on ω_l and the band-gap frequency ω_{cv} is determined by polarizations [Eqs. (21), (A8), and (A9)]. If ω_l is near the gap energy of the material system ω_{cv}, the signal (Rayleigh, Raman, and fluorescence emission) is enhanced. This can be seen from the coefficient to the homogeneity of these equations. Employing a Markov approximation would lead to resonance terms such as $\frac{1}{\gamma + [\omega_{cv} - \omega_l(\pm\omega_{\mathbf{q}})]}$.

$$\partial_t \langle a_v^\dagger a_c b_{\mathbf{q}}^\dagger \rangle_{1+} = -i(-\omega_{\mathbf{q}} - \omega_l + \omega_{cv} - i\gamma)\langle a_v^\dagger a_c b_{\mathbf{q}}^\dagger \rangle_{1+}$$
$$- \frac{i}{\hbar}g_{vc}^q n_{\mathbf{q}}\rho_{vc}^+ - \frac{i}{\hbar}\sum_{\mathbf{k}}D_{cv}^{\mathbf{k}}\langle a_v^\dagger a_v b_{\mathbf{q}}^\dagger c_{\mathbf{k}} \rangle_{1+}$$
$$- \frac{i}{\hbar}\sum_{\mathbf{k}}D_{cv}^{\mathbf{k}}\langle a_c^\dagger a_c b_{\mathbf{q}}^\dagger c_{\mathbf{k}} \rangle_{1+} + \frac{i}{\hbar}\mu_{cv}^-[\langle a_c^\dagger a_c b_{\mathbf{q}}^\dagger \rangle$$
$$- \langle a_v^\dagger a_v b_{\mathbf{q}}^\dagger \rangle], \quad (A8)$$

$$\partial_t \langle a_v^\dagger a_c b_{\mathbf{q}} \rangle_{1+} = -i(\omega_{\mathbf{q}} - \omega_l + \omega_{cv} - i\gamma)$$
$$\times \langle a_v^\dagger a_c b_{\mathbf{q}}^\dagger \rangle_{1+} - \frac{i}{\hbar}g_{vc}^{\mathbf{q}*}[n_{\mathbf{q}} + 1]\rho_{vc}^+$$
$$- \frac{i}{\hbar}\sum_{\mathbf{k}}D_{cv}^{\mathbf{k}}\langle a_v^\dagger a_v b_{\mathbf{q}} c_{\mathbf{k}} \rangle_{1+}$$
$$- \frac{i}{\hbar}\sum_{\mathbf{k}}D_{cv}^{\mathbf{k}}\langle a_c^\dagger a_c b_{\mathbf{q}} c_{\mathbf{k}} \rangle_{1+} + \frac{i}{\hbar}\mu_{cv}^-[\langle a_c^\dagger a_c b_{\mathbf{q}} \rangle$$
$$- \langle a_v^\dagger a_v b_{\mathbf{q}} \rangle]. \quad (A9)$$

Equations (A10)–(A12) describe scattering processes involving two times the laser energy ω_l.

$$\partial_t \langle a_v^\dagger a_c c_{\mathbf{k}} \rangle_{2+} = -i(\omega_k + \omega_{cv} - 2\omega_l - i\gamma)\langle a_v^\dagger a_c c_{\mathbf{k}} \rangle_{2+}$$
$$+ \frac{i}{\hbar}\mu_{cv}^-[\langle a_c^\dagger a_c c_{\mathbf{k}} \rangle_{1+} - \langle a_v^\dagger a_v c_{\mathbf{k}} \rangle_{1+}]$$
$$- \frac{i}{\hbar}\sum_{\mathbf{q}}g_{vc}^{\mathbf{q}}\langle a_v^\dagger a_c b_{\mathbf{q}} c_{\mathbf{k}} \rangle_{2+} - \frac{i}{\hbar}\sum_{\mathbf{q}}g_{cv}^{\mathbf{q}*}\langle a_v^\dagger a_c b_{\mathbf{q}}^\dagger c_{\mathbf{k}} \rangle_{2+}, \quad (A10)$$

$$\partial_t \langle a_v^\dagger a_c b_{\mathbf{q}} c_{\mathbf{k}} \rangle_{2+} = -i(\omega_k + \omega_{cv} + \omega_{\mathbf{q}} - 2\omega_l - i\gamma)$$
$$\times \langle a_v^\dagger a_c b_{\mathbf{q}}^\dagger c_{\mathbf{k}} \rangle_{2+} + \frac{i}{\hbar}\mu_{cv}^-[\langle a_c^\dagger a_c b_{\mathbf{q}} c_{\mathbf{k}} \rangle_{1+}$$
$$- \langle a_v^\dagger a_v b_{\mathbf{q}} c_{\mathbf{k}} \rangle_{1+}] - \frac{i}{\hbar}g_{vc}^{\mathbf{q}*}[n_{\mathbf{q}} + 1]\langle a_v^\dagger a_c c_{\mathbf{k}} \rangle_{2+}, \quad (A11)$$

$$\partial_t \langle a_v^\dagger a_c b_{\mathbf{q}}^\dagger c_{\mathbf{k}} \rangle_{2+} = -i(\omega_k + \omega_{cv} - \omega_{\mathbf{q}} - 2\omega_l - i\gamma)$$
$$\times \langle a_v^\dagger a_c b_{\mathbf{q}}^\dagger c_{\mathbf{k}} \rangle_{2+} + \frac{i}{\hbar}\mu_{cv}^-[\langle a_c^\dagger a_c b_{\mathbf{q}}^\dagger c_{\mathbf{k}} \rangle_{1+}$$
$$- \langle a_v^\dagger a_v b_{\mathbf{q}}^\dagger c_{\mathbf{k}} \rangle_{1+}] - \frac{i}{\hbar}g_{vc}^q n_{\mathbf{q}}\langle a_v^\dagger a_c c_{\mathbf{k}} \rangle_{2+}. \quad (A12)$$

*julia@itp.physik.tu-berlin.de

[1] A. Kaschner, A. Hoffmann, and C. Thomsen, Phys. Rev. B **64**, 165314 (2001).

[2] F. Wang, G. Dukovic, L. E. Brus, and T. F. Heinz, Phys. Rev. Lett. **92**, 177401 (2004).

[3] L. Yang, T. Zhang, A. D. Bristow, S. T. Cundiff, and S. Mukamel, J. Chem. Phys. **129**, 234711 (2008).

[4] A. Sitek and P. Machnikowski, Phys. Rev. B **75**, 035328 (2007).

[5] P. Borri, W. Langbein, S. Schneider, U. Woggon, R. L. Sellin, D. Ouyang, and D. Bimberg, Phys. Rev. B **66**, 081306(R) (2002).

[6] Y. R. Shen, Phys. Rev. B **9**, 622 (1974).

[7] S. Mukamel, *Principles of Nonlinear Optical Spectroscopy* (Oxford University Press, New York, 1995).

[8] H. Rho, L. M. Robinson, N. Mukolobwiez, L. M. Smith, H. E. Jackson, S. Lee, M. Dobrowolska, and J. K. Furdyna, Physica E **11**, 59 (2001).

[9] J. Gomis-Bresco, S. Dommers, V. V. Temnov, U. Woggon, M. Laemmlin, D. Bimberg, E. Malić, M. Richter, E. Schöll, and A. Knorr, Phys. Rev. Lett. **101**, 256803 (2008).

[10] M. Richter, A. Carmele, A. Sitek, and A. Knorr, Phys. Rev. Lett. **103**, 087407 (2009).

[11] R. Heitz, H. Born, A. Hoffmann, D. Bimberg, I. Mukhametzhanov, and A. Madhukar, Appl. Phys. Lett. **77**, 1973 (2000).

[12] W. H. Louisell, *Quantum Statistical Properties of Radiation* (Wiley, New York, 1973).

[13] W. Hayes and R. Loudon, *Scattering of Light by Crystals* (Wiley, New York, 1978).

[14] S. N. Klimin, V. M. Fomin, J. T. Devreese, and D. Bimberg, Phys. Rev. B **77**, 045307 (2008).

[15] R. P. Miranda, M. I. Vasilevskiy, and C. Trallero-Giner, Phys. Rev. B **74**, 115317 (2006).

[16] J. Sue, Y. J. Yan, and S. Mukamel, J. Chem. Phys. **85**, 462 (1986).

[17] M.-R. Dachner *et al.*, Phys. Status Solidi B (to be published).

[18] M. Richter, S. Butscher, M. Schaarschmidt, and A. Knorr, Phys. Rev. B **75**, 115331 (2007).

[19] B. Krummheuer, V. M. Axt, and T. Kuhn, Phys. Rev. B **65**, 195313 (2002).

[20] K. J. Ahn, J. Förstner, and A. Knorr, Phys. Rev. B **71**, 153309 (2005).

[21] O. Stier, M. Grundmann, and D. Bimberg, Phys. Rev. B **59**, 5688 (1999).

[22] The Fröhlich-coupling matrix elements are given by $g_{ii}^q = -i\sqrt{\frac{e^2\omega_{LO}}{2\hbar\epsilon_0 V}}(\frac{1}{\epsilon_\infty}-\frac{1}{\epsilon_s})\frac{1}{q}\langle i|e^{i\mathbf{q}\cdot\mathbf{r}}|i\rangle$.

[23] M. Lindberg, S. An, S. W. Koch, and M. Sargent III, Phys. Rev. A **40**, 4415 (1989).

[24] H. Stolz, *Time-Resolved Light Scattering from Excitons, Vol. 130 of Springer Tracts in Modern Physics* (Springer-Verlag, Berlin, 1994).

[25] M. Kira, F. Jahnke, W. Hoyer, and S. W. Koch, Prog. Quantum Electron. **23**, 189 (1999).

[26] J. H. Eberly and K. Wodkievicz, J. Opt. Soc. Am. **67**, 1252 (1977).

[27] The signal at the detector is given by Eq. (7). In the stationary limit, the detectors time resolution can be set very high. Assuming very long detection times ($\Delta t \rightarrow \infty$), the Gaussians in Eq. (7) become 1 and, after a change of integration variables $t_1 = t' + \tau$ and $t_2 = t'$ Ref. 25 the signal reads, $S(\mathbf{r}, \omega_{k_s}, t) = \int_{-\infty}^{\infty} d\tau \int_0^t dt' \langle E^{(-)}(\mathbf{r}, t'+\tau) E^{(+)}(\mathbf{r}, t')\rangle \times e^{-i\omega_{k_s}\tau}$ The measurement was assumed to last until t, so the integrals limits for t' go from 0 to t. τ is a free parameter and runs from $-\infty$ to ∞ for any value of t'. Evaluating the first integral over t' results in an expression, which is proportional to t, since for a stationary light field, $\langle E^{(-)}(\mathbf{r}, t'+\tau) E^{(+)}(\mathbf{r}, t')\rangle$ does not depend on t'.

[28] A. Thränhardt, S. Kuckenburg, A. Knorr, P. Thomas, and S. W. Koch, Phys. Rev. B **62**, 16802 (2000).

[29] J. Förstner, C. Weber, J. Danckwerts, and A. Knorr, Phys. Status Solidi B **238**, 419 (2003).

[30] M. Kira and S. W. Koch, Phys. Rev. A **73**, 013813 (2006).

[31] W. Vogel and D. Welsch, *Quantum Optics*, 3rd ed. (Wiley-VCH, Berlin, 2006).

[32] *Group IV Elements, IV-IV and III-V Compounds, Vol. III/41b of Landolt-Börnstein—Group III Condensed Matter*, edited by U. Rössler (Springer, New York, 2002).

[33] M. Bagheri Harouni, R. Roknizadeh, and M. H. Naderi, Phys. Rev. B **79**, 165304 (2009).